Suplemento de la Revista Mexicana de Física **3** 0308019 (2022) 1–5

# Meson and glueball spectroscopy within the graviton soft-wall model

Matteo Rinaldi

*Dipartimento di Fisica e Geologia. Università degli studi di Perugia,*
*INFZ section of Perugia, Via A. Pascoli, Perugia, Italy.*

Received 14 January 2022; accepted 9 April 2022

In this contribution we present results of the calculations of several hadronic spectra within the holographic graviton soft-wall (GSW) model. In particular, we studied and compared with data for the ground state and excitations of: glueballs, scalar, vector, axial and pseudo-scalar mesons. The GSW model is found to be capable to describe these observable with only few parameters.

*Keywords:* Graviton soft-wall (GSW).

DOI: https://doi.org/10.31349/SuplRevMexFis.3.0308019

## 1. Introduction

In this contribution we investigate the spectra of some hadronic species. We consider the graviton soft-wall (GSW) model, introduced and applied in Refs. [1-4], initially adopted to describe non perturbative features of glueballs. We remind that the holographic approach relies in a correspondence between a five dimensional classical theory with an AdS metric and a supersymmetric conformal quantum field theory. Since the latter is not QCD, we use the so-called "bottom-up" approach [5-7]. where the five dimensional classical theory is properly modified to reproduce non-perturbative QCD properties as much as possible. Furthermore, the GSW model is a modification of the initial soft-wall (SW) where a dilaton field is introduced to softly break conformal invariance. In GSW model, in order to properly describe the scalar glueball spectrum, a modification of the metric has been proposed. This model has been successfully applied to reproduce non perturbative features of mesons and glueballs [1,7-10]. In particular, we calculated and impressively described the spectra of: glueballs (with even and odd spin), the light and heavy scalar mesons, the $\rho$, the $a_1$, the $\eta$ and the $\pi$. Moreover, we showed in Ref. [3] that only when the masses of the glueballs and the mesons are close, mixing is to be expected [11]. However, if this mass condition is associated to a different dynamics, mixing will not happen [12].

## 2. Essential features of the GSW model

The essential difference between the GSW model from the traditional SW one, is a deformation of the $AdS$ metric in 5 dimensions:

$$\begin{aligned} ds^2 &= e^{\alpha\phi_0(z)} g_{MN} dx^M dx^N \\ &= \frac{R^2}{z^2}\left(\eta_{\mu\nu} dx^\mu dx^\nu - dz^2\right), \end{aligned} \tag{1}$$

where $g_{MN}$ is the AdS$_5$ metric and $\phi_0(z) = k^2 z^2$ [1,8-10,13,14]. Modifications of the metric have been also proposed in other studies of the properties of mesons and glueballs within AdS/QCD [8,14-22]. The action, in the gravity sector, written in terms of the standard AdS metric of the SW model, is:

$$\begin{aligned} \bar{S} = \int d^5 x e^{\phi_0(z)\left(\frac{5}{2}\alpha-\beta+1\right)} \\ \times e^{-\phi_n(z)} \sqrt{-g} e^{-\phi_0(z)} \mathcal{L}(x_\mu, z)\,. \end{aligned} \tag{2}$$

In the GSW model, the parameter $\alpha$ encodes the effects due to the modification of the metric, while, $\beta$ is used to recover the SW results as much as possible. Indeed, $\beta$ is not a free parameter and it is fixed to lead the SW kinematic term in the action [1,3,4]. For example, for scalar fields $\beta = \beta_s = 1 + \frac{3}{2}\alpha$ and for a vector $\beta = \beta_v = 1 + (1/2)\alpha$. In Ref. [2], an additional dilaton $\phi_n$ has been also phenomenologically proposed to describe scalar and pseudo-scalar mesons in order to obtaina binding potential in the equation of motion. We anticipate that this quantity does not contain any free parameter, which are namely $\alpha$ and $k$. In closing, in order to properly take into account the chiral symmetry breaking, essential to describe the pion spectrum, a modification of the dilaton has been proposed.

## 3. The glueball spectra within the GSW model

In this section we discuss and present the GSW predictions for the glueball spectra with even and odd spins together with the successful comparison with lattice data.

### 3.1. Scalar glueballs

Here we recall the main results discussed in Ref. [1]. We remind that in this case, the GSW model predicts that the scalar glueball is described by its dual graviton which is a solution of the Einstein equation (Ee) for a perturbation the metric (1). The linearized Ee can be rearranged in a Schrödinger like equation:

$$-\frac{d^2\phi(t)}{dt^2} + \left(\frac{8}{t^2}e^{2t^2} - 15t^2 + 14 - \frac{17}{4t^2}\right)\phi(t) = \Lambda^2\phi(t). \tag{3}$$

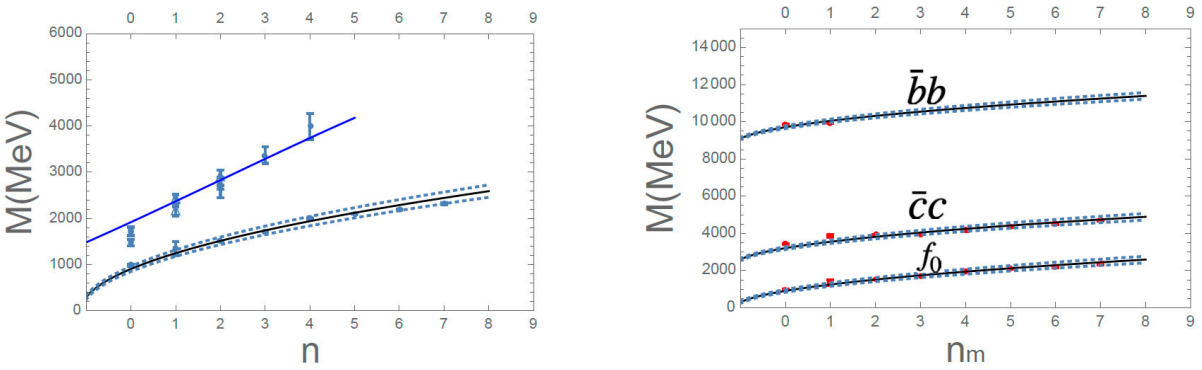


FIGURE 1. Left panel: GSW fit to the scalar lattice glueball spectrum [40-42] and to the experimental scalar meson spectrum [35,36]. Solid line for $\alpha$: 0.55 and $0.55 \pm 0.04$ (dotted). Right panel: The scalar meson spectrum GSW fit to the data shown for all quark sectors. Experimental data [35,36]. The curves correspond to $C_c = 2400$ MeV for the $c\bar{c}$ mesons and $C_b = 8700$ MeV for the $b\bar{b}$ mesons.

where, as usual, we assumed factorization between the $z$ and $x_\mu$ dependence, $t = \sqrt{\alpha k^2/2}\ z$ and $\Lambda^2 = (2/\alpha k^2)\ M^2$, being $M$ the mode mass.

It is remarkable that the potential is uniquely determined by the metric and its modification. The only free parameter is the scale factor depending on $\alpha k^2$. This term is fixed from the comparison with lattice QCD [1]. As one can see in the left panel of Fig. 1, for $\alpha k^2 \sim (0.37\ \text{GeV})^2$ the linear glueball spectrum is well reproduced, at variance with the SW model. We also stress the good agreement with the graund state mass obtained by the BESIII data of the $J/\Psi$ decays [23,24] (SDTK) very recently, after analysis.

### 3.2. Spin dependent glueball spectra

We found out that the ground state of glubealls with spin is well reproduced if we consider the approach of Refs. [8,20,25] to describe spin effects. In this case the action is that of a scalar field [4]:

$$\bar{S} = \int d^5x\ \sqrt{-g} e^{-k^2z^2} \Big[ g^{MN} \partial_M G(x) \partial_N G(x) + \quad (4)$$
$$+ e^{\alpha k^2 z^2} M_5^2 R^2 G(x) \Big] ,$$

and the spin dependence is encoded in the 5-dimensional mass term: $i)$ $M_5^2R^2 = J(J+4)$ for even spin $J$ and $ii)$ $M_5^2R^2 = (J+2)(J+6)$ for odd spin $J$. One should notice that since $M_5^2R^2 \geq 0$, the potential in equation of motion is binding and therefore no additional dilatons are needed. Results of the calculations for the odd and even glueballs are shown in Tables I-II, respectively. As one can see, results are

TABLE I. Comparison of the masses of the ground states for the odd spin glueballs (in MeV).

| $J^{PC}$ | My [38] | Li [26] | Our Work [2] |
|---|---|---|---|
| $1^{--}$ | $3240 \pm 480$ | 395 | $3308 \pm 15$ |
| $3^{--}$ | $4330 \pm 460$ | 4150 | $4451 \pm 12$ |
| $5^{--}$ | | 5050 | $5752 \pm 10$ |

TABLE II. Same of Table I for even glueballs.

| $J^{PC}$ | My [38] | Gy [39] | Our Work [2] |
|---|---|---|---|
| $2^{++}$ | $2150 \pm 130$ | $2620 \pm 50$ | $2695 \pm 21$ |
| $4^{++}$ | $3640 \pm 150$ | | $3920 \pm 14$ |
| $6^{++}$ | $4360 \pm 460$ | | $5141 \pm 12$ |

in fairly agreement with data. We also evaluated and compared the Regge trajectories provided by the GSW model with lattice data. In general, the form is $J \sim a_g M^2 + b_g$, where $g = o$ stands for odd spin and $g = e$ is referred to even spin, respectively. In the odd case: $a_o = 0.18 \pm 0.01,\ b_o = -0.75 \pm 0.28$ [2], in agreement with $J \sim 0.18M^2 + 0.25$ [26]. For even glueballs: $a_e = 0.21 \pm 0.01,\ b_e = 0.58 \pm 0.34$ [2] in agreement with $J \sim 0.25M^2$ [27,28].

## 4. Meson spectroscopy

Here we show the main results for the spectroscopy of the $f_0$, heavy scalar, $\rho$, $a_1$, $\eta$ and pion mesons. We stress again that for the latter case a modification of the dilaton $\phi_0$ must be included to incorporate chiral symmetry breaking.

### 4.1. Light and heavy scalar mesons

In this case the action is that of Eq. (4) but since now $M_5^2R^2 = -3$, the relative potential is not binding. Therefore, at variance to the the glubeall case, the additional contribution $\exp[-\phi_n(z)]$ must be included. Details on this topic are presented in Ref. [2]. Here we mention that $\phi_n$ is chosen to produce in the potential a term proportional to the expansion, up to the second order, of $\exp(\alpha k^2 z^2)$ and thus preserving the binding feature. By keeping fixed $\alpha k^2 = 0.37\ \text{GeV}^2$, we found a reasonable good fit, see left panel of Fig. 1, for $0.51 \leq \alpha \leq 0.59$. In the case of heavy mesons we added the quark mass contribution to the light scalar masses [2,4] in order to effectively include the dynamics the mass of the heavy quarks [29-31]. In particular, the heavy mass ($M_h$) is obtained from the previous light scalar mass ($M_l$) as follows:

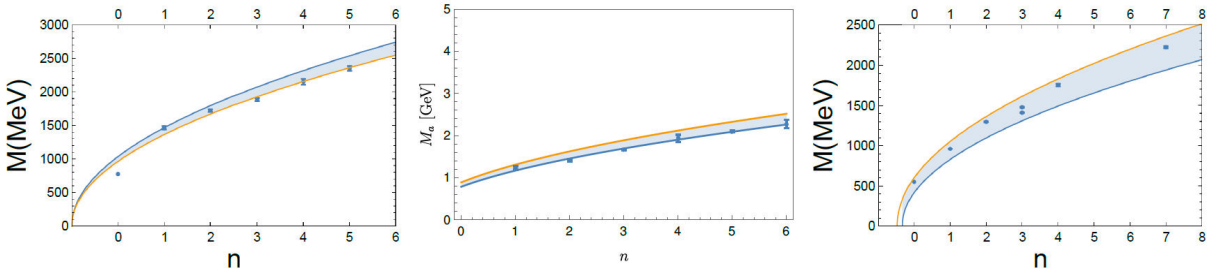


FIGURE 2. Left: The $\rho$ mass plot as a function of mode number. Experimental data [35,36]. Center panel, the $a_1$ spectrum. Data from Refs. [34,36]. Right panel, the $\eta$ spectrum. Data from Refs. [35,36]

$M_h = M_h + C$, where $C$ is the contribution of the quark masses. $C_c = 2400$ MeV, for the $c\bar{c}$ mesons, and for the $b\bar{b}$ mesons $C_b = 8700$ MeV. The successful comparison with data [4] is displayed in the left and right panels of Fig. 1. One should notice that $C_c$ and $C_b$ are comparable with the values of $2m_c$ and $2m_b$, respectively, as expected.

### 4.2. The $\rho$ spectrum

For the $\rho$ meson, the action is equal to that of a vector field within the usual SW model since $M_5^2 R^2 = 0$ [20]:

$$\bar{S}=-\frac{1}{2}\int d^5x\,\sqrt{-g}\,e^{-k^2z^2}\left[\frac{1}{2}g^{MP}g^{QN}F_{MN}F_{PQ}\right]. \quad (5)$$

In this case, there is no need of the auxiliary dilaton since $M_5^2 R^2 = 0$ and thus the potential is binding. As one can see in the left panel of Fig. 2, the agreement is good, exception is $\rho(770)$. Such a discrepancy suggests that the GSW model must be further improved.

### 4.3. The $a_1$ axial meson spectrum

In the case of the axial-vector mesons, due to chiral symmetry breaking, $M_5^2 R^2 = -1$ [32,33]. Therefore the EoM for the $a_1$ can be obtained from the action of a vector field with a conformal mass different from zero:

$$\bar{S} = -\frac{1}{2}\int d^5x\sqrt{-g}e^{-k^2z^2-\phi_n}\left[\frac{1}{2}g^{MP}g^{QN}F_{MN}F^{PQ} + M_5^2R^2g^{PM}A_PA_Me^{\alpha k^2z^2}\right]. \quad (6)$$

Since in this case $M_5^2 R^2 < 0$, the corresponding potential is not binding and a modification of the dilaton is required. Details on the differential equation defining the contribution are included in Ref. [2]. With the parameters previously addressed, we get the spectrum shown in the central panel of Fig. 2. Our calculation favors that the $a_1(1930), a_1(2095)$ and $a_1(2270)$ are axial resonances [34]. Moreover, the agreement is even more impressive if a missing ground state with a mass lower then the quoted 1230 MeV will be observed.

### 4.4. The $\eta$ pseudo-scalar meson

The EoM is similar to that of the scalar case but now, $M_5^2 R^2 = -4$ [33]. As expected, one needs to include the additional dilaton to get a binding potential. In the right panel of Fig. 2 we show our calculation of the spectrum, we remind that the band stands for the theoretical error on $\alpha\ \alpha = 0.55 \pm 0.04$. The comparison with the experimental data [35,36] is very good also in this case. Moreover, the GSW model predicts that $\eta(1405)$ and $\eta(1475)$ are degenerate, as discussed in PDG review. Moreover, since in the upper mass sector the experimental mass gap is larger, the GSW model also favors: *i)* the existence of two resonances between the $\eta(1760)$ and the $\eta(2225)$ and $ii)$ that the $\eta(1405)$ and $\eta(1470)$ are the same resonance. We recall that the results for the $\rho,\ a_1$ and $\eta$ masses are free parameter calculations.

### 4.5. The pion spectrum

In the case of the pion, the Goldstone boson of SU(2) x SU(2) chiral symmetry, as already anticipate, we need to incorporate in the model chiral symmetry breaking mechanism. Since, as discussed in *e.g.*, Refs. [9,15,37], the physics of confinement and chiral symmetry breaking could ascribed to the dilaton [9,15,37], we propose a modification of the dilaton profile function [2], we consider:

$$\phi_0(z) = \beta_s \tanh(\gamma z^4 + \delta)k^2z^2. \quad (7)$$

The parameter $\tanh(\delta)$ is responsible for the the chiral symmetry breaking, see details in Ref. [2]. This choice preserves the large $z$ behaviour, which leads to Regge trajectory of the higher mode spectrum. On the other hand, the low $z$ region describes the transition region and $\delta$ and $\gamma$ incorporates the effects of the spontaneous chiral symmetry breaking. Also in this case, in analogy with the $\eta$, we need to include $\phi_n$ to get a binding potential. The pion spectrum is shown in the Table III compared with the PDG data [35,36]. The predicts more pion states the experimentally observed [33,37].

## 5. Glueball-Meson mixing

Here we discuss the conditions for a not favorable mixing, *i.e.* states with mostly gluonic valence structure [3]. We consider an holographic light-fron (LF) representation of the EoM in term of the Hamiltonian [5]

$$H_{LC}|\Psi_k>= M^2|\Psi_k>, \quad (8)$$

TABLE III. Experimental results for the $\pi$ masses given by the PDG particle listings [35,36] compared with our calculations, $\delta = 1.5235$. The masses in MeV.

| | $\pi^0$ | | $\pi(1300)$ | | | $\pi(1800)$ |
|---|---|---|---|---|---|---|
| PDG | $134.9768 \pm 0.0005$ | | $1300 \pm 100$ | | | $1819 \pm 10$ |
| Our work [2] | 135 | $943 \pm 111$ | $1231 \pm 133$ | $1463 \pm 151$ | $1663 \pm 168$ | $1842 \pm 183$ |

and a two dimensional Hilbert space generated by a meson and a glueball states, $\{|\Psi_m>, |\Phi_g>\}$. Mixing occurs when the hamiltonian is not diagonal in the subspace. A matrix representation of the hamiltonian is given by

$$[H] = \begin{pmatrix} m_1 & \alpha \\ \alpha & m_2 \end{pmatrix}, \tag{9}$$

where $\alpha =< \Psi_m|H|\Phi_g >$, $m_1 =< \Psi_m|H|\Psi_m >$ and $m_2 =< \Phi_g|H|\Phi_g >$. We are assuming $m_2 > m_1$ and for simplicity $\alpha$ real and positive. After diagonalization the eigenstates have a mass $M_\pm = m \pm \sqrt{\alpha^2 + (\Delta m)^2}$, where $m = (m_1 + m_2)/2$ and $\Delta m = (m_2 - m_1)/2$. The first physical meson, assuming to be the lightest one, is given by the eigenvector of $H$ [3]. Since we fixed the meson spectrum to the experimental values, $|\Psi_{phy}>$ represents a physical meson state while we have fixed the glueball spectrum to the lattice values, therefore the glueball state is our initial state $|\Phi_g>$, thus

$$|<\Psi_{phy}|\Phi_g>|^2 = \frac{\alpha^2}{(M_- - m_2)^2}. \tag{10}$$

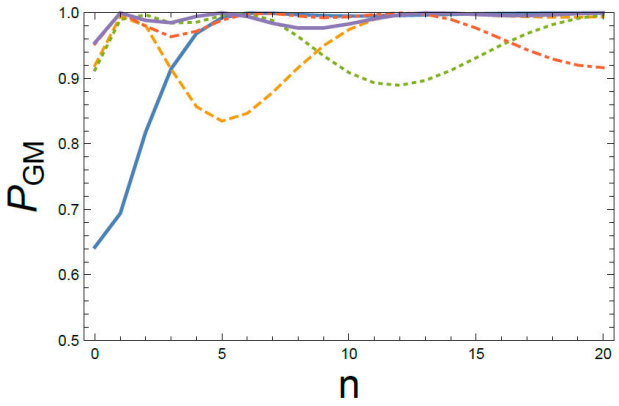


FIGURE 3. The probability of no mixing for the glueball with mode numbers $n_g = 0$ (solid),1 (dashed), 2 (dotted), 3 (dot-dashed), 4 (solid) as a function of meson mode number $n$.

The mixing probability is proportional to the overlap of these two wave functions (w.f.). We calculate the probability for no mixing, *i.e.*, $P_{GM} = 1 - |\langle\Psi_{phy}|\Phi_g\rangle|^2$. As one can see in Fig. 3, the the mixing should occur when $n_g = 2, 3, 4$ and the meson mode numbers $n \sim 10, 13, 17$. This condition reduces the overlap probability for mixing dramatically. Therefore, we predict the existence of almost pure glueball states, in the scalar sector, in the mass range above 2 GeV.

## 6. Conclusions

In this contribution we presented the applications of the GSW model to the glueball and meson spectra. We saw that the proposed modification of the metric is fundamental to reproduce experimental data with only two parameters. We propose the inclusion of an additional free parameter dilaton to get binding potential for tachionic 5-dimensional masses. Excellent agreements with data are found. For the pion, the SW dilaton has been properly modify to describe the chiral symmetry breaking in the model. Also in this case the comparison with data is quite good. We conclude by remarking the capability of the model in reproducing several masses of very different hadronic systems with only few universal parameters and therefore leading to a relevant predicting power.

## Acknowledgements

This work was supported, in part by the STRONG-2020 project of the European Unions Horizon 2020 research and innovation programme under grant agreement No 824093. The author thank the organizers of the “19th International Conference on Hadron Spectroscopy and Structure (HADRON2021)”.

1. M. Rinaldi and V. Vento, Scalar and Tensor Glueballs as Gravitons. *Eur. Phys. J. A* **54** (2018) 151.
2. M. Rinaldi and V. Vento, Meson and glueball spectroscopy within the graviton soft wall model. *Phys. Rev. D* **104** (2021) 034016.
3. M. Rinaldi and V. Vento, Pure glueball states in a Light-Front holographic approach. *J. Phys. G* **47** (2020) 055104.
4. M. Rinaldi and V. Vento, Scalar spectrum in a graviton soft wall model. *J. Phys. G* **47** (2020) 125003.
5. S. J. Brodsky and G. F. de Teramond, Light-front hadron dynamics and AdS/CFT correspondence. *Phys. Lett. B* **582** (2004) 211-221.

6. L. Da Rold and A. Pomarol, Chiral symmetry breaking from five dimensional spaces. *Nucl. Phys. B* **721** (2005) 79-97.
7. A. Karch, E. Katz, D. T. Son, and M. A. Stephanov, Linear confinement and AdS/*QCD. Phys. Rev. D* **74** (2006) 015005.
8. E. Folco Capossoli and Henrique Boschi-Filho, Glueball spectra and Regge trajectories from a modified holographic softwall model. *Phys. Lett. B* **753** (2016) 419-423.
9. J. Erlich, E. Katz, D. T. Son, and M. A. Stephanov, QCD and a holographic model of hadrons. *Phys. Rev. Lett.* **95** (2005) 261602.
10. P. Colangelo, F. De Fazio, F. Giannuzzi, F. Jugeau, and S. Nicotri, Light scalar mesons in the soft-wall model of AdS/QCD. *Phys. Rev. D* **78** (2008) 055009.
11. V. Vento, Scalar glueball spectrum. *Phys. Rev. D,* **73** (2006) 054006.
12. V. Vento, Glueball-Meson Mixing. *Eur. Phys. J. A* **52** (2016) 1.
13. G. F. de Teramond and S. J. Brodsky, Hadronic spectrum of a holographic dual of QCD. *Phys. Rev. Lett.* **94** (2005) 201601.
14. P. Colangelo, F. De Fazio, F. Jugeau, and S. Nicotri, On the light glueball spectrum in a holographic description of QCD. *Phys. Lett. B* **652** (2007) 73-78.
15. A. Vega and P. Cabrera, Family of dilatons and metrics for AdS/QCD models. *Phys. Rev. D* **93** (2016) 114026.
16. T. Akutagawa, K. Hashimoto, and T. Sumimoto, Deep Learning and AdS/QCD. *Phys. Rev. D* **102** (2020) 026020.
17. T. Gutsche, V. E. Lyubovitskij, I. Schmidt, and A. Yu Trifonov, Mesons in a soft-wall AdS-Schwarzschild approach at low temperature. *Phys. Rev. D* **99** (2019) 054030.
18. I. R. Klebanov and J. Martin Maldacena, Superconformal gauge theories and non-critical superstrings. *Int. J. Mod. Phys. A* **19** (2004) 5003-5016.
19. M. A. Martin Contreras and A. Vega, Different approach to decay constants in AdS/QCD models. *Phys. Rev. D* **101** (2020) 046009.
20. E. Folco Capossoli, M. A. Martin Contreras, D. Li, A. Vega, and H. Boschi-Filho, Hadronic spectra from deformed AdS backgrounds. *Chin. Phys. C* **44** (2020) 064104.
21. A. E. Bernardini, N. R. F. Braga, and R. da Rocha, Configurational entropy of glueball states. *Phys. Lett. B* **765** (2017) 81-85.
22. D. Li and M. Huang, Dynamical holographic QCD model for glueball and light meson spectra. *JHEP*, **11** (2013) 088.
23. A. V. Sarantsev, I. Denisenko, U. Thoma, and E. Klempt, Scalar isoscalar mesons and the scalar glueball from radiative J= decays. *Phys. Lett. B*, **816** (2021) 136227.
24. E. Klempt. Scalar mesons and the fragmented glueball. 4 (2021)
25. H. Boschi-Filho, N. R. F. Braga, and H. L. Carrion, Glueball Regge trajectories from gauge/string duality and the Pomeron. *Phys. Rev. D* **73** (2006) 047901.
26. F. J. Llanes-Estrada, Pedro Bicudo, and Stephen R. Cotanch, Oddballs and a low odderon intercept, *Phys. Rev. Lett.*, **96** (2006) 081601.
27. P. V. Landshoff, Pomerons, In Elastic and diffractive scattering. Proceedings, 9th Blois Workshop, Pruhonice, *Czech Republic*, **2001** (2001) 161-171.
28. H. B. Meyer and M. J. Teper, Glueball Regge trajectories and the pomeron A Lattice study. *Phys. Lett. B* **605** (2005) 344-354.
29. T. Branz, T. Gutsche, V. E. Lyubovitskij, I. Schmidt, and A. Vega, Light and heavy mesons in a soft-wall holographic approach. *Phys. Rev. D* **82** (2010) 074022.
30. Y. Kim, J.-P. Lee, and S. Houng Lee, Heavy quarkonium in a holographic QCD model. *Phys. Rev. D* **75** (2007) 114008.
31. S. S. Afonin and I. V. Pusenkov, The quark masses and meson spectrum A holographic approach. *Phys. Lett. B* **726** (2013) 283-289
32. S. He, M. Huang, Q.-S. Yan, and Y. Yang, Confront Holographic QCD with Regge Trajectories. *Eur. Phys. J. C* **66** (2010) 187-196.
33. M. A. Martin Contreras, A. Vega, and S. Cortes, Light pseudoscalar and axial spectroscopy using AdS/QCD modified soft wall model. *Chin. J. Phys.* **66** (2020) 715-723.
34. A. V. Anisovich *et al*., Partial wave analysis of anti-p p annihilation channels in flight with I = 1, C = +1. *Phys. Lett. B* **517** (2001) 261-272.
35. M. Tanabashi *et al*., Review of Particle Physics. *Phys. Rev. D* **98** (2018) 030001.
36. P. A. Zyla *et al*., Review of Particle Physics. *PTEP* **2020** (2020) 083C01.
37. T. Gherghetta, J. I. Kapusta, and T. M. Kelley, Chiral symmetry breaking in the soft-wall AdS/QCD model. *Phys. Rev. D* **79** (2009) 076003.
38. H. B. Meyer, Glueball regge trajectories. PhD thesis, Oxford U. (2004)
39. E. Gregory *et al*., Towards the glueball spectrum from unquenched lattice QCD. *JHEP*, **10** (2012) 170.
40. C. J. Morningstar and M. J. Peardon, The Glueball spectrum from an anisotropic lattice study. *Phys. Rev. D* **60** (1999) 034509.
41. Y. Chen *et al*., Glueball spectrum and matrix elements on anisotropic lattices. *Phys. Rev. D* **73** (2006) 014516.
42. B. Lucini, M. Teper, and U. Wenger, Glueballs and k-strings in SU(N) gauge theories Calculations with improved operators. *JHEP*, **06** (2004) 012.